Journal of Engineering Physics and Thermophysics, Vol. 78, No. 4, 2005

HYDRODYNAMICS IN TECHNOLOGICAL PROCESSES

COMPARATIVE ANALYSIS OF THE VORTEX HEAT EXCHANGE IN TURBULENT FLOWS AROUND A SPHERICAL HOLE AND A TWO-DIMENSIONAL TRENCH ON A PLANE WALL

S. A. Isaev,[a] A. I. Leont'ev,[b] G. I. Kiknadze,[c] N. A. Kudryavtsev,[a] and I. A. Gachechiladze[c]

UDC 532.517.4:621.1.016.4

The vortex heat exchange in turbulent flows around a spherical hole and a transverse trench, identical in depth and in the shape of the middle cross section, on a plane wall has been numerically investigated using multiblock computational technologies. A factorized, implicit multiblock algorithm and a Menter's model of shear-stress transfer were tested in the process of comparative analysis of calculation and experimental data on flows around isolated holes.

The problem of intensification of heat exchange in flows around holes is of considerable interest for specialists in thermal physics. In recent years, the geography of investigations on this problem has widened sharply. At present, practically all countries of the world are involved in them. The interest shown in the method of vortex intensification of heat exchange in flows is evidently explained by the fact that this method makes it possible to increase the heat transfer from a wall at low hydraulic losses. However, this process has been predominantly investigated by experimental methods that give no way of obtaining an integral idea of its physical mechanisms. Such an idea can be obtained using numerical-simulation methods, which have been rapidly developing in recent years.

The present work continues a series of investigations [1–10] devoted to numerical simulation of the convective heat exchange in turbulent flows of an incompressible fluid around isolated holes and an ensemble of holes of various depth and shape on a plane with account for the blocking of the flow by the walls of a narrow channel. In this case, prominence is given to the interrelation between the restructuring of self-organizing vortex structures and the intensification of heat exchange in the neighborhood of holes.

Considerable recent advances have been made in the numerical study of the jet-vortex structures responsible for the vortex intensification of heat exchange in three-dimensional separation flows around holes. An analysis of the evolution of a vortex flow around an isolated spherical hole, included in a narrow channel, on a wall with increase in the depth of the hole has shown that the two-vortex flow in the shallow hole is spasmodically transformed into a single-vortex structure with diagonal transfer of fluid in a deep hole. This transformation is accompanied by a jump-like increase in the heat transfer from both the hole itself and the wake downstream of it. It has been established that such transformation of the near-wall flow and the heat-exchange can also take place in shallow holes if they are asymmetric. One of the technologically simplest holes is a hole representing two hemispheres connected by a cylinder. Such an elongated hole can be arbitrarily oriented relative to an incoming flow. It was positioned at an angle of 45^{o} to an incoming flow in calculations and experiments. An analysis of flows around spherical and conical holes has shown that the heat transfer in them increases as a result of intensification more rapidly than the hydraulic losses. It has been established that three-dimensional vortex flows in such holes are synchronized, which allows the important conclusion that, in them, there arises an ordered near-wall vortex layer determining the high heat-exchange characteristics of the

[a]Academy of Civil Aviation, 38 Pilotov Str., St. Petersburg, 196620, Russia; email: isaev@SI3612.spb.edu; [b]N. E. Bauman Moscow State Technical University, Moscow, Russia; [c]BASERT Company, Moscow, Russia. Translated from Inzhenerno-Fizicheskii Zhurnal, Vol. 78, No. 4, pp. 117–128, July–August, 2005. Original article submitted May 11, 2004.

1062-0125/05/7804-0749

curvilinear surface of the indicated holes around which the stream flows. However, a limited number of holes were investigated in the earlier works, and these investigations were not systematic in character. As a matter of fact, there are still many outstanding questions in the problem considered. We have attempted to answer to some of them in the present paper.

First and foremost, it is interesting to compare the behavior of two-dimensional and three-dimensional turbulent vortex flows around holes identical in shape but different in depth on a smooth surface and the heat exchange in them. Our main concern was with the gradient zone downstream of a trench or a hole, in which a three-dimensional flow provides a high level of heat transfer. Note that the behavior of a turbulent flow and the heat exchange in the neighborhood of a trench with an envelope in the form of a circular arc with rounded edges at the site of connection with a plane wall has been analyzed in detail in [11].

Methodology of Numerical Simulation of Turbulent Heat Exchange. The vortex flow and heat exchange in the neighborhood of curvilinear reliefs were calculated using Reynolds equations [12] closed in accordance with the model of shear-stress transfer [13] and energy equations by the implicit finite-volume method on a set of partially intersecting, different-scale, structured block grids of simple topology. The multiblock approach allows one to correctly represent characteristic, different-scale physical elements on a corresponding grid. The initial equations written in increments of dependent variables were solved in computational cells in accordance with the concept of splitting by physical processes, and the velocity and pressure fields were determined using the SIMPLEC algorithm. The parameters in the connected cells positioned at the points of intersection of grids and in the near-boundary regions were calculated using linear interpolation. The multiblock algorithm realized in a special VP2/3 program package (velocity–pressure, two-dimensional and three-dimensional versions) was verified in the process of solving a number of two-dimensional and three-dimensional problems having experiential analogs.

Multiblock computational technologies used for solving three-dimensional problems of vortex hydromechanics and thermal physics have been systematically developed over the last five years. Of the available works on comparative analysis of experimental and calculation data on the flows investigated, we considered publications devoted to simulation of a low-velocity air flow in a rectangular channel with a circular vortex cell [14], an asymmetric separation flow around a cylinder with a disk positioned before its face [15], and the vortex dynamics and convective heat exchange in laminar [16] and turbulent flows around a spherical hole on a plane [5, 6], a channel [17], and a set of spherical holes in a plane-parallel narrow channel [7]. In [18], the calculation data on the temperature regime in a railroad tunnel of an underground railway, realized in the case of fire in a train carriage, were compared with the analogous measurement data obtained at the All-Union Scientific-Research Institute of Fire Protection. These works allow the conclusion that, by and large, the multiblock strategy is acceptable for solving complex engineering problems on personal computers with very small computational resources.

Formulation of the Problem. Three-dimensional and plane turbulent flows of an incompressible viscous fluid and the convective heat exchange in the region near a plane wall with a spherical hole or a circular trench with a middle cross section in the form of a circle were calculated. The diameter of the hole (the width of the trench) d, representing the distance between the points of its connection with the plane wall, was taken as the characteristic linear size of the problem (Fig. 1a). The determining linear sizes — the depth of the hole (trench) Δ, the radius of the rounding of the sharp-pointed edge r, the initial thickness of the boundary layer δ, and the sizes of the computational region — were determined in fractions of d. The velocity of an incompressible viscous fluid flowing uniformly at a distance from the wall U was taken as the scale of de-dimension of the parameters. The Reynolds number determined by U and d in the process of parametric investigation of the effect of Δ was equal to $4 \cdot 10^4$, which corresponds to the experimental value of Re determined in [19]. The Prandtl number for air was taken to be 0.7, and the turbulent Prandtl number was taken to be 0.9.

The computational region ABCD (Fig. 1b) includes a part of the wall with trench AD, around which the stream flows, on which the adhesion conditions are set. The temperature of the heated wall is maintained constant and equal to 377 K. The parameters are fixed at the input boundary AB. The velocity profile is equal to 1/7 at the initial thickness of the boundary layer δ. The flow above this layer is uniform, i.e., $u = 1$. The energy of turbulent pulsations in this region comprises 1.5% of the turbulence energy of typical wind tunnels. The scale of turbulence is of the order of the trench width (hole diameter). The parameters of turbulence in the boundary layer were determined using the tra-

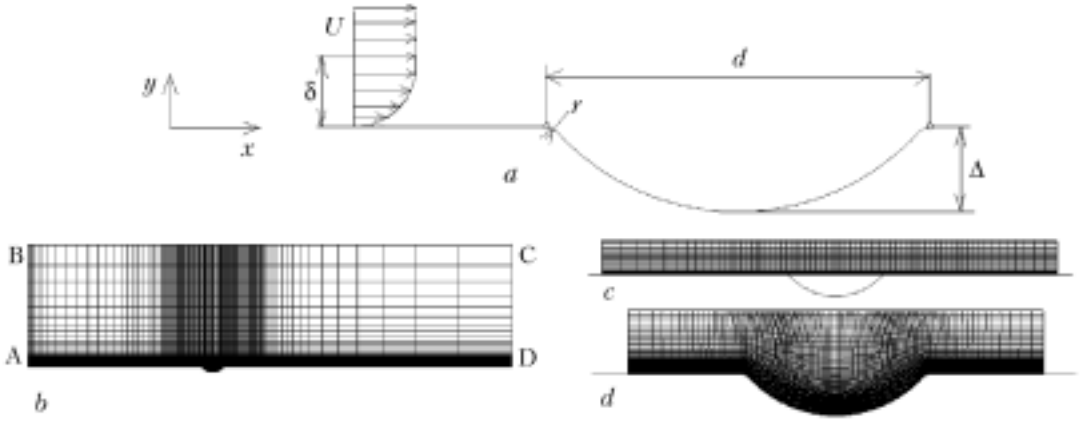

Fig. 1. Diagram of a trench (hole) on a plane wall with designations (a) and multiblock computational grids: b) external Cartesian grid, c) internal Cartesian grid, and d) trench grid.

ditional Prandtl model of mixing. The temperature of the isothermal incoming flow was maintained at the "room" level and was equal to 293 K. This temperature was taken as the characteristic temperature.

"Soft" boundary conditions (the conditions of continuation of solution) were set at output boundaries BC and CD. The flow boundaries were positioned at a fairly large distance from the hole (trench); the distance from them was determined on the assumption that the parameters of the flow in the neighborhood of the concavity have a small influence on the characteristics of the flow near the indicated boundaries.

The sizes of the computational module in the horizontal and vertical directions were equal to 17 and 5.175 respectively. The vertical size of the near-wall subregion, in which the turbulent boundary layer of initial thickness 0.05 was calculated, was 0.175. The distance from the trench to the input boundary was taken to be equal to six.

The multiblock grid (Fig. 1b–d) used for calculating, e.g., a flow around a trench of depth 0.22, consisted of three grids different in scale and structure. The first of them (Fig. 1b) is a Cartesian grid with nonuniform pitches in the longitudinal and transverse directions and a bunching to the wall and the neighborhood of the trench; it contains 129×48 cells and covers the whole computational region. The second grid (Fig. 1c) was constructed for representation of the near wake downstream of the trench; it represents a near-wall Cartesian grid consisting of 68×33 cells and covers the trench neighborhood of size 4×0.175. The third grid, representing a curvilinear grid similar to an orthogonal grid, was calculated in the process of solving elliptic equations; it is consistent with the trench surface, contains 133×54 cells, and covers the trench zone of size 1.8×0.175. The near-wall pitch was 0.0005 in the parametric calculations; however, it was varied in the range 10^{-4}–$5 \cdot 10^{-4}$ in the process of testing.

The three-dimensional problem on a flow around a spherical hole of diameter d and depth Δ (in fractions of d) is similar in formulation to the corresponding two-dimensional problem [11]. The only addition is the boundary conditions for the transverse velocity component w. Soft boundary conditions are set at the side boundaries of the computation region of size $16 \times 5.175 \times 12.77$ (in the case where the distance from the region with a hole to the input boundary is equal to six).

For the purpose of comparison of the calculation data obtained with experimental data [19], we considered flows around three shallow holes (of depth ~0.06) close in configuration and one deep hole (of depth ~0.22) at one and the same Reynolds number, equal to $4 \cdot 10^4$.

For the first shallow hole ($\Delta = 0.06$, $r = 0.1$, $\delta = 0.05$), the problem was solved on the assumption that the flow is symmetric relative to the geometric plane of symmetry that passes through the center of the hole and is parallel to the velocity at the input to the region (Fig. 2a and b). In this case, the fluid motion and the heat exchange in the neighborhood of the hole were determined in a semispace, i.e., with a double economy of the computational resources, which is very important for an ensemble of holes. Of course, this assumption should be substantiated. However, preliminary numerical investigations of flows around holes, carried out as early as the middle 1990s within the framework of the simplified approach to the simulation of flows on a multiblock Cartesian grid with the use of a two-parameter dissipation model of turbulence [1, 2], demonstrated the acceptability of using the symmetry plane for cal-

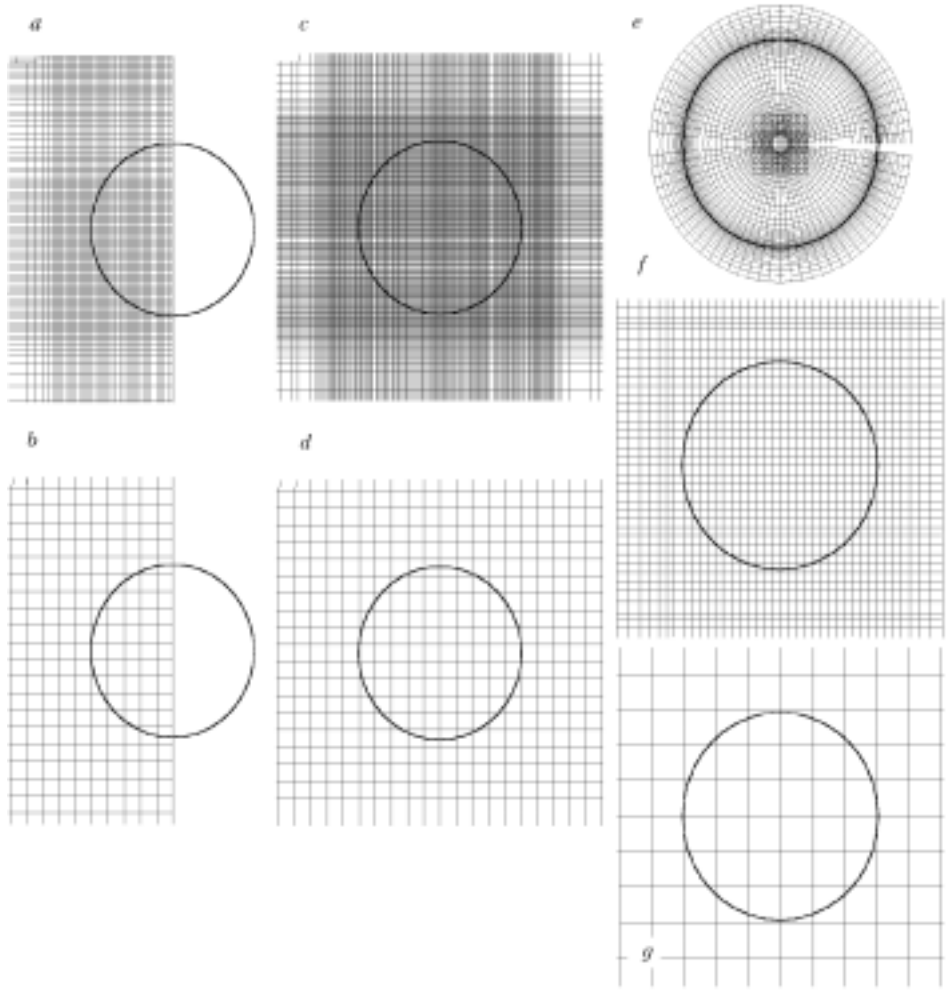

Fig. 2. Multiblock grids used in methodical calculations of three shallow holes of depth 0.06 (a, b — semispace with a central symmetry plane), 0.0625 (c, d), and 0.062 (e, f, g): a, c, f) time grids covering the holes; b, d, g) external Cartesian grids for digitization of the computational region; e) cylindrical grid with a rectangular axial patch surrounding the hole.

culating flows around shallow holes. The multiblock computational grid used in the first case includes an external rectangular grid containing $68 \times 46 \times 28$ cells and an internal grid containing $140 \times 69 \times 49$ cells bunching near the hole and in the wake downstream of it; constructed in the subregion of height 0.15, width 1.75, and length (along x) 4.5 with an origin at the point with coordinates $x = -1.5$, $y = z = 0$. The minimum pitches along the horizontal and vertical coordinates of the internal grid were equal to 0.02, and the near-wall pitch was equal to 10^{-4}. The velocity components were calculated with an accuracy of 10^{-5}.

In the second computational variant ($\Delta = 0.0625$, $r = 0.1$, $\delta = 0.05$), the hole was considered as a part of a relief without introduction of the simplified assumption on the flow symmetry (Fig. 2c and d). The dimensions of the computational region were such as in the first case. The multiblock computational grid also included two grids: an external Cartesian grid containing $68 \times 38 \times 55$ cells and an internal grid with $157 \times 32 \times 171$ cells. The minimum pitch of the grid along the coordinates x and y in the region of the hole was equal to 0.01, and the near-wall pitch was $5 \cdot 10^{-4}$.

The flow around the third hole ($\Delta = 0.062$, $r = 0.21$, $\delta = 0.042$) was calculated on four intersecting grids (Fig. 2e, f, and g): an external Cartesian grid ($51 \times 43 \times 33$ cells), an internal grid surrounding the hole and the wake

TABLE 1. Effect of the Scheme and Geometric Factors on the Experimental Values of the Local Parameters of a Flow around a Plane Wall with a Spherical Hole and the Characteristics of Turbulence, and the Integral Force and Thermal Characteristics of the Flow at Re = 10^4

Parameters	$\Delta = 0.06,\ h = 10^{-4}$	$\Delta = 0.0625,\ h = 5\cdot10^{-4}$	$\Delta = 0.062,\ h = 8.3\cdot10^{-5}$	$\Delta = 0.22,\ h = 5\cdot10^{-4}$
p_{max}	0.0689	0.0714	0.0768	0.1116
p_{min}	–0.0981	–0.1054	–0.0935	–0.1246
u_{max}	1.031	1.031	1.034	1.027
u_{min}	–0.0295	–0.0509	–0.0438	–0.2133
v_{max}	0.1226	0.1258	0.1251	0.2672
v_{min}	–0.0702	–0.07026	–0.0741	–0.113
w_{max}	0.086	0.1403	0.1347	0.2112
w_{min}	–0.1315	–0.1403	–0.1347	–0.143
k_{max}	0.01004	0.0113	0.01089	0.04454
$\nu_{t,max}$	0.00101	0.00097	0.00099	0.002877
$C_{xf\mathrm{tr}}$	0.003478	0.00300	0.00312	0.001164
$C_{xp\mathrm{tr}}$	0.001123	0.00194	0.00189	0.01242
$C_{x\mathrm{tr}}$	0.004603	0.00494	0.00501	0.01359
$Nu_{tr}/Nu_{pl,tr}$	0.975	0.977	0.975	1.12
$C_{xf\mathrm{c}}$	0.004084	0.003913	0.004001	0.004004
$Nu_c/Nu_{pl,c}$	1.012	0.995	1.014	1.177

TABLE 2. Dependence of the Local, Extremum, and Integral Characteristics of the Flow and the Heat Exchange in the Neighborhood of a Trench and a Hole on Their Depth (Diagrams of the elements around which the stream flows are presented in fig. 5)

Parameters	Depth			
	0.0625		0.22	
	trench	hole	trench	hole
p_{max}	0.0817	0.0714	0.0815	0.1116
p_{min}	–0.08615	–0.1054	–0.0826	–0.1246
u_{max}	1.028	1.031	1.025	1.027
u_{min}	–0.0619	–0.0509	–0.2165	–0.2133
v_{max}	0.1168	0.1258	0.1985	0.2672
v_{min}	–0.0549	–0.07026	–0.0974	–0.113
w_{max}	—	0.1403	—	0.2112
w_{min}	—	–0.1403	—	–0.143
k_{max}	0.0135	0.0113	0.0333	0.04454
$\nu_{t,max}$	0.00133	0.00097	0.00217	0.00288
$C_{xf\mathrm{tr}}$	0.00183	0.00300	–0.00043	0.00116
$C_{xp\mathrm{tr}}$	0.00417	0.00194	0.0148	0.01242
$C_{x\mathrm{tr}}$	0.00600	0.00494	0.0144	0.01359
$Nu_{tr}/Nu_{pl,tr}$	1.007	0.977	1.19	1.12
$C_{xf\mathrm{c}}$	0.00382	0.00391	0.0038	0.00400
$Nu_c/Nu_{pl,c}$	1.052	0.995	1.25	1.177

subregion (51 × 36 × 51 cells), a cylindrical grid around the hole (76 × 34 × 37 cells), and a rectangular "axis patch" (17 × 34 × 17 cells). The near-wall pitch was taken to be equal to $8.3\cdot10^{-5}$.

Analysis of Results. Some of the results of calculations carried out on the three above-mentioned grids are presented in Figs. 3–8 and in Tables 1 and 2.

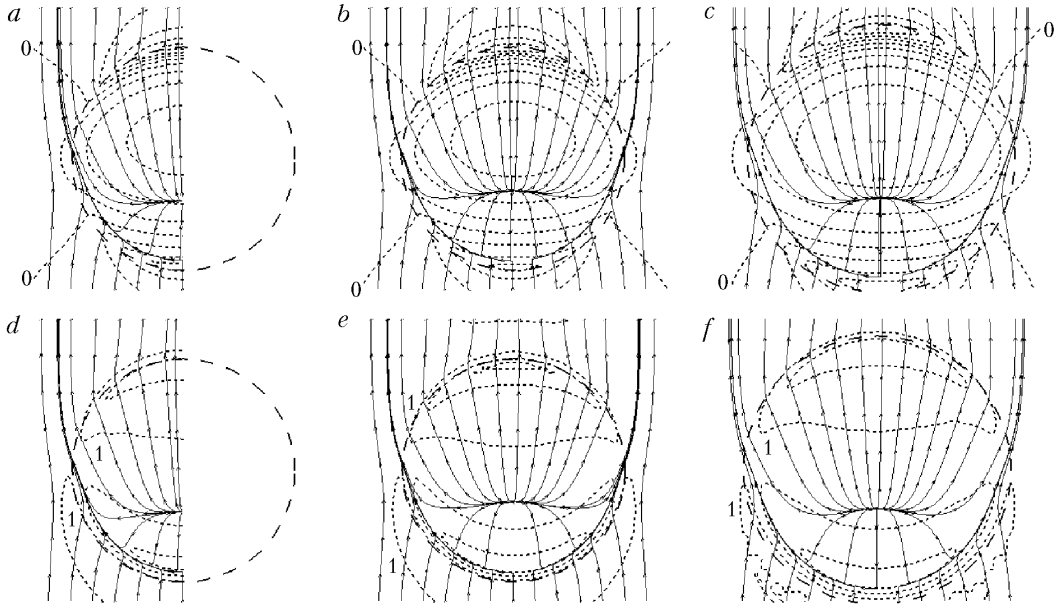

Fig. 3. Comparison of the patterns of flows around shallow holes of close depth on a plane wall [a, d) $\Delta = 0.06$; b, e) 0.0625; c, f) 0.062], fields of surface isobars drawn with a step of 0.02 from the zero level (a, b, c), and fields of surface isolines of relative heat transfer Nu/Nu_{pl} drawn with a step of 0.025 from the unit level (d, e, f). The dashed line denotes the edges of the hole.

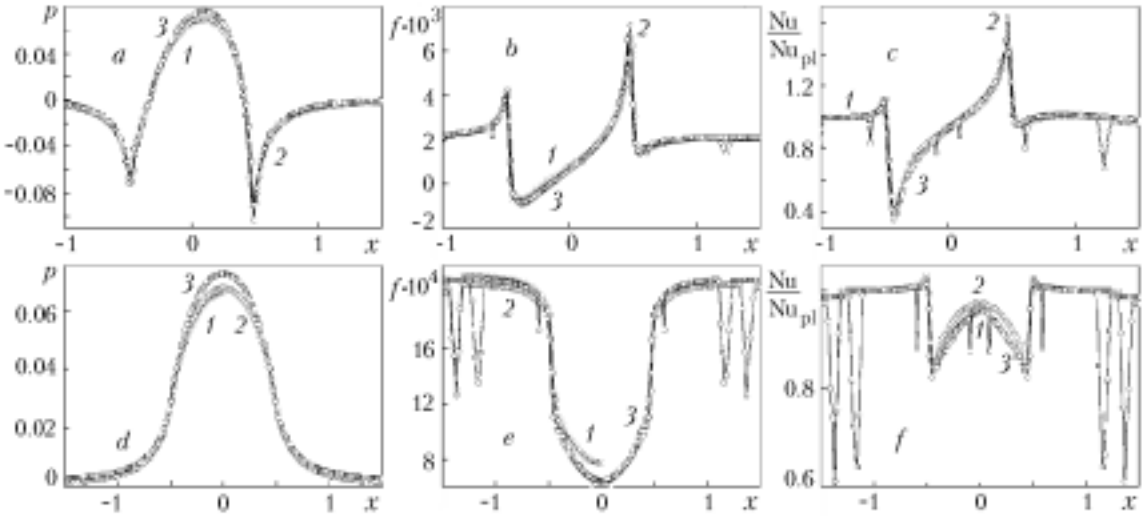

Fig. 4. Comparative analysis of the surface distributions of excess pressure (a, d), friction stress (b, e), and relative heat transfer (c, f) in the longitudinal [a, b, c) $z = 0$] and transverse [d, e, f) $x = 0$] middle cross sections of the hole: 1) $\Delta = 0.06$; 2) 0.0625; 3) 0.062.

The methodical calculations of turbulent flows around shallow holes close in depth and the convective heat exchange in their neighborhood have shown that the topology of multiblock grids has an insignificant influence on the results of numerical simulation. It is significant that the data obtained with the use of simplified grids, e.g., Cartesian grids (see Fig. 2a and c) that take no account of the shape of the smoothed edges of spherical holes, correlate fairly well with analogous data obtained with cylindrical grids consistent with the hole surface around which the stream flows (Fig. 2e). Moreover, the results of numerical simulation remained practically unchanged when the near-wall pitch

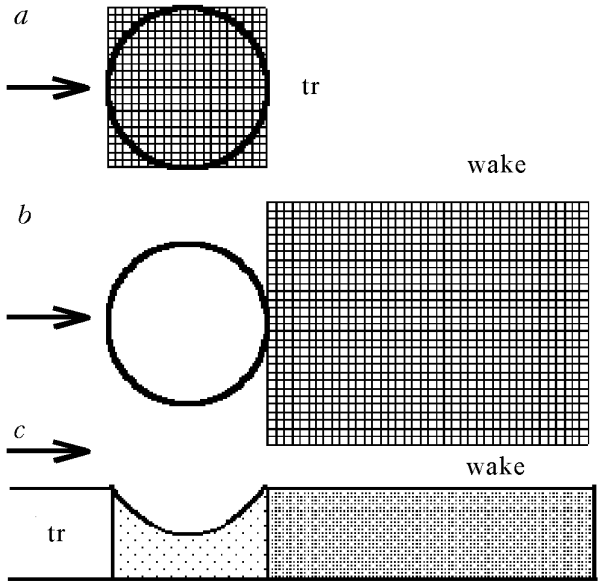

Fig. 5. Diagrams of the concavity (tr) and the wake zone (wake) on the surface around which the stream flows in the three-dimensional (a, b) and two-dimensional (c) cases.

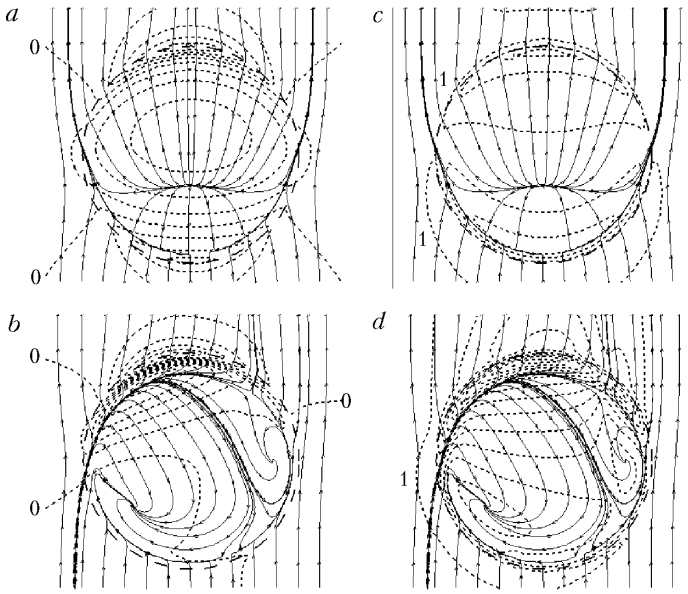

Fig. 6. Comparative analysis of the patterns of fluid spreading on the surface of a shallow hole [$\Delta = 0.0625$ (a, c) and a deep hole [$\Delta = 0.22$ (b, d)] represented by isobars drawn with a step of 0.02 from the zero level of the excess pressure (a, b) and isolines of relative heat transfer Nu/Nu_{pl} (c, d) drawn with a step of 0.025.

h changed in the range considered from 10^{-4} to $5 \cdot 10^{-4}$, which indicates that calculations can be performed with a coarse pitch near the wall.

As was noted in [8], a flow around a spherical hole occupies surrounding near-wall layers, i.e., the lines of flow are bent on its side slopes. Such behavior of the flow is explained by the fact that the excess pressure decreases upstream of the concavity, which also leads to an acceleration of the flow. This is especially true for a flow without separation around a shallow hole.

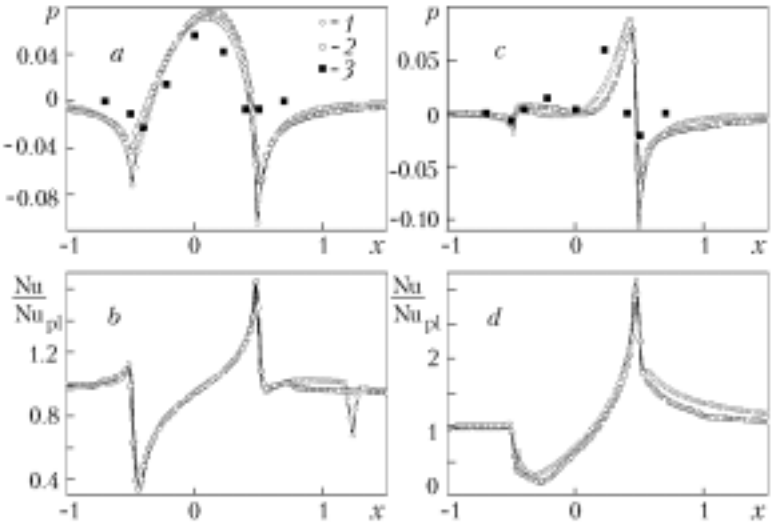

Fig. 7. Graphs of longitudinal distribution of excess pressure (a, c) and local relative heat transfer Nu/Nu_{pl} (b, d) in the middle cross section of the neighborhood of a hole (1) and a trench (2, 3). The experimental data (3) were taken from [19].

The deceleration of the flow in a shallow hole (Δ is of the order of 0.06) leads to the formation of a thin separation bubble as in the case of flow in a trench of the same depth [11], and the line of connection lies somewhat higher than the concavity center (Fig. 6a). In fact, on the pattern of fluid spreading inside the hole, this line represents a line of distributed sources, from which some fluid particles move to meet the incoming flow, and the behavior of the oppositely directed trajectories of particles, covering the windward slope, is analogous to the behavior of a jet flowing from a nozzle. As a result, within the hole there arises a fairly compact three-dimensional region of return-circulatory fluid motion with a circumferential separation line lying on the leeward slope somewhat lower than the leading edge of the hole.

The dome-like distribution of the static pressure points to a fairly high excess pressure, whose maximum is shifted below the center of the hole to the windward side. It should be noted that the pressure decreases fairly rapidly outside the side edges of the hole (Fig. 4d) and, beyond its areal, whose diameter can be equal to the four diameters of the hole, the excess pressure is close to zero.

The fluid flowing from the concavity to the plane makes a sharp turn, which leads to a peak pressure drop. The rarefaction zone, i.e., the zone where the excess pressure is low, has dimensions (in both the longitudinal and transverse directions) of the order of one diameter. The zone where the flow is accelerated, with the result that the friction stress increases sharply (by two times) (Fig. 4b), is fairly narrow and is limited to the neighborhood of the concavity-edge rounding. It is interesting that the maximum rarefaction in the wake downstream of a hole is much higher than that downstream of a trench. This is most probably due to the transverse reduction of the flow to the geometric plane of symmetry, which is illustrated (Fig. 6a) by the turn of the streamlines downstream of the trailing edge of the spherical hole. As a consequence, in the case of a three-dimensional flow, the relative heat transfer downstream of the concavity decreases with a smaller rate (Fig. 7b).

It has been established in the present work, as also in earlier works [3, 4, 8], that in a flow around a deep hole (Δ of the order of 0.2) there arise single-vortex structures (Fig. 6b and d) transporting the fluid in the transverse direction with a maximum velocity of the order of 0.2. It should be noted that the predicted pattern of the flow correlates well with experimental data (see, e.g., [20]). It is evident that the space topology of a turbulent flow around a deep spherical hole differs radically from that of a flow around a trench of the same depth on a plane, even through the distributions of the static pressure in the middle cross section and the intensity of the reverse flow are practically identical in the two-dimensional and three-dimensional cases (Table 2). However, a spherical hole turbulizes the flow much more strongly. It was found that the maximum levels of turbulent energy and vortex viscosity for it are approximately 25% higher than those for a transverse trench. The reverse situation is observed for a shallow hole: the maxi-

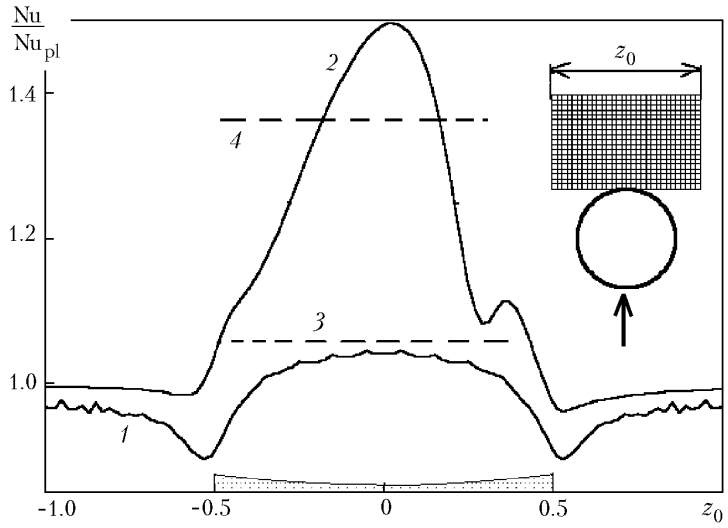

Fig. 8. Comparative analysis of the relative heat transfer averaged over a unit-length band in the transverse direction in the wake downstream of a concavity: 1, 2) holes; 3, 4) trenches; 1, 3) $\Delta = 0.0625$; 2, 4) $\Delta = 0.22$. The edges of the concavity are shown.

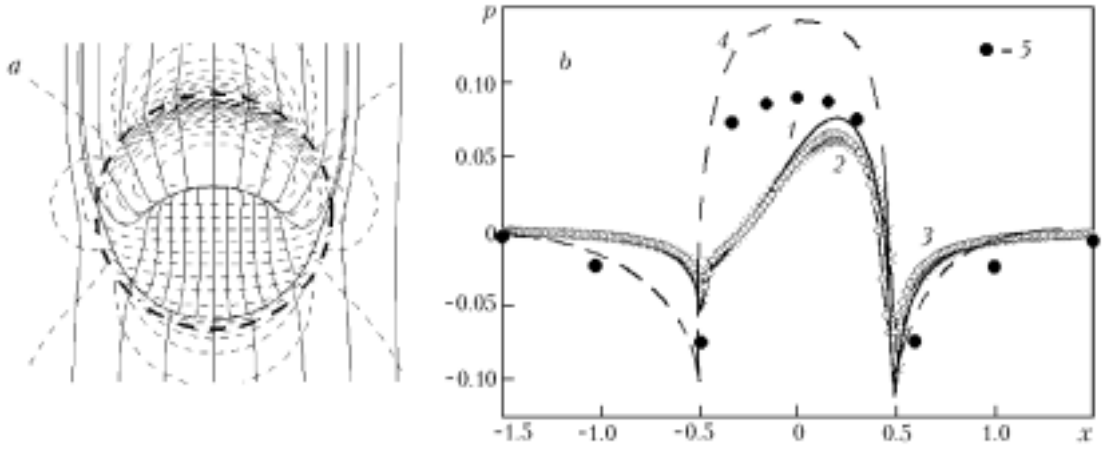

Fig. 9. Pattern of fluid spreading on the surface of a shallow hole ($\Delta = 0.083$; $r = 0.1$, $\delta = 0.05$) represented by isobars drawn with a step of 0.01 (a) and comparative analysis of the calculated and experimental distributions of the static pressure in the transverse middle cross section of a hole (b): $r = 0.1$ and $\delta = 0.05$ (1), 0.25 and 0.1 (2), 0.01 and 0.175 (3); 4) data obtained using the potential theory; 5) experiment [20, 22].

mum turbulence characteristics of this hole are smaller by the same value than those in the two-dimensional case, i.e., the near-wall flow is turbulized with a delay.

It is seen from the data (Table 2) of numerical analysis of the intensification of heat exchange in a hole and in the wake downstream of it, performed using the method of rectangular elements around which the stream flows [6, 8, 9, 21], that two-dimensional concavities offer advantages over the three-dimensional ones in relative heat transfer. On the one hand, this is a consequence of the choice of a fairly long element in the wake (two characteristic linear sizes), and on the other hand the width of the band downstream of the hole, taken to be equal to 1.5, seems to be incorrect. This, of course, is not of critical importance when holes of different depth are compared; however, in the case of concavities of different dimension, a different method of analysis should be used. Figure 8 shows the data on the relative heat transfer averaged over a unit length of the band downstream of the hole. This allows one to deter-

TABLE 3. Comparative Analysis of the Integral, Extremum, and Local Characteristics of a Flow around a Hole of Depth 0.083 for Different Geometric, Regime, and Scheme Parameters

Parameters	$r = 0.1$, $\delta = 0.05$, Cartesian two-block grids ~950,000 cells, $h = 5\cdot10^{-4}$	$r = 0.25$, $\delta = 0.1$, Cylindrical Cartesian grids ~300,000 cells, $h = 5\cdot10^{-4}$	$r = 0.01$, $\delta = 0.175$, Cylindrical Cartesian grids ~132,000 cells, $h = 5\cdot10^{-4}$	$r = 0.1$, $\delta = 0.05$, Cylindrical Cartesian grids ~600,000 cells, $h = 10^{-4}$
p_{max}	0.0766	0.0657	0.061	0.068
p_{min}	–0.0111	–0.0696	–0.132	–0.098
u_{max}	1.030	1.014	1.015	1.017
u_{min}	–0.102	–0.0927	–0.0893	–0.090
v_{max}	0.158	0.132	0.146	0.150
v_{min}	–0.0482	–0.0445	–0.046	–0.0495
w_{max}	0.155	0.121	0.152	0.147
w_{min}	–0.155	0.121	–0.152	–0.147
k_{max}	0.01916	0.01645	0.0149	0.0165
$\nu_{t,max}$	0.000992	0.00144	0.00152	0.00146
$C_{xf\text{tr}}$	0.002296	0.00221	0.00179	0.00219
$C_{xp\text{tr}}$	0.00419	0.00317	0.00364	0.00361
$C_{x\text{tr}}$	0.00649	0.00538	0.00543	0.00579

mine the functional dependence of Nu/Nu_{pl} on the band width z_0 and compare it with the corresponding value of Nu/Nu_{pl} for a unit-length element in the wake downstream of a trench. For a shallow spherical hole, only the relative heat transfer in the middle cross section of the wake downstream of the hole approaches the heat transfer in the plane case. At the same time, in a deep hole there is a zone of width comprising approximately 40% of the hole diameter, in which the heat transfer is markedly higher (by 14% at the most) than that in the two-dimensional hole.

The distributions of the local characteristics in the longitudinal cross section inside a shallow concavity and its integral characteristics were found to be practically identical to those in the plane and three-dimensional cases. Despite the significantly inhomogeneous distribution of the relative heat transfer in the hole (Fig. 4c and f), the total heat transfer in it is equal to that of a plane wall. As for a deep hole, the transverse transport of the fluid in it substantially weakens (by 7%) the intensification of the heat exchange (Table 2) as compared with that in a trench. However, the heat transfer increases by 12% in this hole and by 18% in the near wake downstream of it.

Yet, one experiment on a flow around an isolated shallow hole of depth 0.083 is frequently described in the literature [20, 22]. The distributions of the pressure measured in the longitudinal middle cross section of the hole are compared with the estimates made on the basis of the potential theory. Since the conditions of the physical experiment are not concretized and the shape of the hole, which is determined not only by its relative depth but also by the surface curvature, including the radius of the rounding of the sharp-pointed edge, is not known, in our numerical experiment we used several spherical holes close in configuration and different in the thickness of the boundary layer. A comparative analysis of the data of calculations of flows around holes having different geometric, regime, and design parameters is presented in Fig. 9 and in Table 3. The Reynolds number was taken to be equal to $4\cdot10^4$.

The comparatively small differences between the characteristics presented in Table 3 can be due to the differences between the initial parameters.

The conclusions made are somewhat paradoxical because the simplified shape of the hole used in the calculations on Cartesian grids just differs substantially from a sphere (especially at the rounded edges). This difference is apparently responsible for the somewhat overstated (by 15%) profile drag of the hole calculated using Cartesian grids, which allows us to recommend the inclusion of insets, describing the smoothed edges of holes, into multiblock grids. At the same time, the surface-pressure distributions (Fig. 9b) in holes of different configurations are very close, especially in maximum pressure peak (independently of the boundary-layer thickness and the radius of the rounding). However, the minimum pressure, realized immediately downstream of the hole, depends substantially on r. At very small r, the pressure drop p_{min} is significant. Analysis of the fluid-spreading patterns presented in Fig. 9a shows that a small

increase in the depth of a shallow hole (from 0.0625 to 0.083) leads to a marked increase in the dimensions of the separation zone (the point of connection of the flow is brought to the windward side of the hole); however, the type of hole remains the same in this case, i.e., it continues to be a separation bubble.

Comparison of the numerical-simulation data with predictions made on the basis of the potential theory and the experimental data allows a number of interesting conclusions. The difference between the shapes of the pressure diagrams has engaged our attention first of all. Curves 1–3 with peaks shifted to the windward side differ radically from the canonical pressure distribution (curve 4) characteristic of potential flows. It is somewhat strange that the experimental data of [20, 22] correspond to the latter, but, even so, they partially correspond (in extremum values) to the calculation data. This is most probably due to the use of the potential theory, the applicability of which to a near-wall viscous-fluid flow of the type of a boundary layer seems to be controversial. The quantitative disagreement between the indicated data supports this conclusion. At the same time, the satisfactory agreement between the results of numerical and physical experiments is evidence of the acceptability of the multiblock computational method and the Menter's model of shear-stress transfer selected.

In conclusion, we present data on the efficiency of the VP2/3 multiblock computational complex as applied to the calculation of test variants of flows around a spherical hole on a plane wall. A separation flow around a hole of depth 0.1 (r = 0.25) at Re = 10^4 and at an initial boundary-layer thickness of 0.175 has been numerically simulated on a set of four different-scale grids (three Cartesian grids and one cylindrical grid) with a total number of cells of ~135,000. The calculations were performed on a Pentium IV computer with a processor of speed 1.7 GHz and took 94.5 min, which is entirely acceptable for conducting serial parametric calculations.

Thus, the multiblock algorithm realized in the special VP2/3 package has been verified and the Menter's model of shear-stress transfer has been tested on the basis of comparison of the calculation data with the available experimental data on the pressure distribution in the middle cross section of shallow and deep spherical holes. Comparison of a spherical hole and a trench, as elements of the vortex intensification of heat exchange, shows that the heat transfer in a three-dimensional concavity of depth 0.22 is one-and-a-half times higher than the heat transfer from a plane wall and 10% higher than the heat transfer from a unit zone in the wake downstream of a trench. However, the region of the hole where the heat transfer exceeds the heat transfer in the trench is very narrow (of the order of 0.4).

This work was carried out with financial support from the Russian Basic Research Foundation (project Nos. TO2P-015, 02-02-17562, 04-02-81005, 02-01-01160, 05-02-16184, and 05-01-00162).

NOTATION

C_{xp} and C_{xf}, coefficients of profile and friction resistance; c_p, heat capacity at a constant pressure, kJ/(kg·K); d, diameter of the hole, m; f, friction stress related to the doubled kinetic head in fractions of ρU^2; h, near-wall pitch in fractions of d; k, energy of turbulent pulsations in fractions of U^2; n, coordinate measured along the normal to the profile in fractions of d; Nu, Nusselt number determined as $d\theta/dn$; OTL, kinematic-viscosity coefficient; p, pressure related to the doubled kinetic head in fractions of ρU^2; Pr, Prandtl number, Pr = $c_p\mu/\lambda$; r, radius of the rounding of the sharp-pointed edge in fractions of d; Re, Reynolds number, Re = $\rho UD/\mu$; T, temperature, K: U, velocity of a uniform flow, m/sec; u, v, and w, longitudinal, vertical, and transverse components of the velocity vector in fractions of U; x, y, z, Cartesian coordinates, m; δ, initial thickness of the boundary layer in fractions of d; Δ, depth of the concavity in fractions of d; ε, rate of turbulent-energy dissipation in fractions of U^3/d; λ, heat-conductivity coefficient, W/(m·K); μ, viscosity, Pa·sec; ν, kinematic viscosity, μ/ρ; θ, dimensionless temperature; $\theta = (T - T_w)/(T_{inlet} - T_w)$; ρ, density, kg/m^3; ω, specific rate of turbulent energy dissipation in fractions of U/d. Subscripts: inlet, parameters at the inlet to the computational region; min and max, minimum and maximum values; pl, parameters on a plane without a hole; t, turbulent; tr, concavity zone (trench zone); wake, wake region; w, parameters on a wall; 0, transverse size of the unit-length zone downstream of the hole.

REFERENCES

1. S. A. Isaev, V. B. Kharchenko, and Ya. P. Chudnovskii, Calculation of a three-dimensional flow of a viscous incompressible liquid in the neighborhood of a shallow hole on a plane surface, *Inzh.-Fiz. Zh.*, **67**, Nos. 5–6, 373–378 (1994).

2. S. A. Isaev, A. I. Leont'ev, and A. E. Usachov, Methodological aspects of numerical simulation of the dynamics of vortex structures and heat transfer in viscous turbulent flows, *Izv. Ross. Akad. Nauk*, *Énergetika*, No. 4, 140–148 (1996).
3. S. A. Isaev, A. I. Leont'ev, and P. A. Baranov, Identification of self-organizing tornado-like structures in numerical simulation of a turbulent incompressible fluid flow around a hole on a plane, *Pis'ma Zh. Tekh. Fiz.*, **26**, Issue 1, 28–35 (2000).
4. S. A. Isaev, A. I. Leont'ev, and P. A. Baranov, Bifurcation of a vortex turbulent flow and intensification of heat transfer in a hole, *Dokl. Ross. Akad. Nauk*, **373**, No. 5, 615–617 (2000).
5. S. A. Isaev, A. I. Leont'ev, Kh. T. Metov, and V. B. Kharchenko, Simulation of the influence of the viscosity on the tornado heat exchange in a turbulent flow around a small hole on a plane, *Inzh.-Fiz. Zh.*, **75**, No. 4, 98–104 (2002).
6. P. A. Baranov, S. A. Isaev, A. I. Leont'ev, A. V. Mityakov, V. Yu. Mityakov, and S. Z. Sapozhnikov, Physical and numerical simulation of vortex heat transfer in a turbulent flow around a spherical hole on a plane, *Teplofiz. Aéromekh.*, **9**, No. 5, 521–532 (2002).
7. S. A. Isaev, A. I. Leont'ev, P. A. Baranov, I. A. Pyshnyi, and A. E. Usachov, Numerical analysis of the vortical intensification of heat transfer in a channel with a package of deep spherical holes on one of its walls, *Dokl. Ross. Akad. Nauk*, **386**, No. 5, 621–623 (2002).
8. S. A. Isaev, A. I. Leont'ev, P. A. Baranov, and I. A. Pyshnyi, Numerical analysis of the influence of the depth of a spherical hole on a plane wall on the turbulent heat exchange, *Inzh.-Fiz. Zh.*, **76**, No. 1, 52–59 (2003).
9. S. A. Isaev and A. I. Leont'ev, Numerical simulation of the vortical intensification of heat transfer in a turbulent flow around a spherical hole on the wall of a narrow channel, *Izv. Ross. Akad. Nauk*, *Teplofiz. Vys. Temp.*, **41**, No. 5, 755–770 (2003).
10. R. Banker, M. Ya. Belen'kii, M. A. Gotovskii, S. A. Isaev, and B. S. Fokin, Experimental and theoretical study of the hydrodynamics and heat transfer in a plane channel of variable width for the cases of smooth and intensified surfaces, in: *Proc. IIIrd Russian Nat. Conf. on Heat Transfer*, Vol. 6, *Enhancement of Heat Transfer. Radiative and Combined Heat Transfer* [in Russian], MÉI, Moscow (2002), pp. 37–40.
11. S. A. Isaev, P. A. Baranov, N. A. Kudryavtsev, and A. E. Usachov, Analysis of the vortex heat transfer in a flow around a trench on a plane using multiblock computation technologies and different semi-empirical models of turbulence, *Inzh.-Fiz. Zh.*, **77**, No. 6, 152–161 (2004).
12. A. V. Ermishin and S. A. Isaev (Eds.), *Control of Flows around Bodies with Vortex Cells as Applied to Flying Vehicles of Integral Arrangement* (*Numerical and Physical Modeling*) [in Russian], MGU, Moscow (2003).
13. F. R. Menter, M. Kuntz, and R. Langtry, Ten years of industrial experience with the SST turbulence model, in: K. Hanjalic, Y. Nagano, and M. Tummers (Eds.) *Turbulence*, *Heat and Mass Transfer*, Begell House, New York (2003).
14. P. A. Baranov, S. V. Guvernyuk, M. A. Zubin, and S. A. Isaev, Numerical and physical simulation of a circulation flow in a vortex cell on the wall of a plane-parallel channel, *Izv. Ross. Akad. Nauk*, *Mekh. Zhidk. Gaza*, No. 5, 44–56 (2000).
15. P. A. Baranov, S. V. Guvernyuk, S. A. Isaev, and V. B. Kharchenko, Simulation of a laminar flow around a cylinder with a coaxial front disk at small and moderate angles of attack by multiblock computational technologies, *Aéromekh. Gaz. Dinam.*, No. 1, 16–27 (2003).
16. S. A. Isaev, A. I. Leont'ev, Kh. T. Metov, and V. B. Kharchenko, Numerical analysis of the effect of the viscosity on the vortex dynamics in a laminar separation flow around a hole on a plane with allowance for its asymmetry, *Inzh.-Fiz. Zh.*, **74**, No. 2, 62–67 (2001).
17. S. A. Isaev, I. A. Pyshnyi, A. E. Usachov, and V. B. Kharchenko, Test of a multiblock computational technology in calculating laminar and turbulent flows around a spherical hole on the wall of a channel, *Inzh.-Fiz. Zh.*, **75**, No. 5, 122–124 (2002).
18. P. A. Baranov, A. D. Golikov, S. A. Isaev, and A. Yu. Snegirev, Numerical and physical simulation of the thermal regime in a railroad tunnel of an underground railway in the case of fire in a moving train carriage, *Inzh.-Fiz. Zh.*, **73**, No. 5, 918–921 (2000).

19. V. N. Afanas'ev, V. Yu. Veselkin, A. I. Leont'ev, A. P. Skibin, and Ya. P. Chudnovskii, Hydrodynamics and Heat Transfer in a Flow around Individual Recesses on an Initially Smooth Surface [in Russian], Preprint No. 2-91, Pts. 1 and 2, N. É. Bauman Moscow State Technical University, Moscow (1991).
20. V. V. Alekseev, I. A. Gachechiladze, G. I. Kiknadze, and V. G. Oleinikov, Tornado-like energy transfer on three-dimensional concave reliefs — structure of self-organizing flows, their visualization and mechanisms of flows around surfaces, in: *Proc. II Russian Nat. Conf. on Heat Transfer*, Vol. 6, *Intensification of Heat Transfer. Radiative and Combined Heat Transfer* [in Russian], MÉI, Moscow (1998), pp. 33–42.
21. S. A. Isaev, Development of multiblock computational technologies for solving the problem on vortex aeromechanics and thermal physics, in: *Proc. XIV School-Seminar of Young Scientists and Specialists headed by Academician of the Russian Academy of Sciences A. I. Leont'ev "Problems of Gas Dynamics and Heat and Mass Transfer in Power Plants"* [in Russian], Vol. 1, MÉI, Moscow (2003), pp. 13–16.
22. I. A. Gachechiladze, G. I. Kiknadze, G. L. Korolev, V. G. Oleinikov, and V. P. Rogankov, Calculation of flows around three-dimensional concavities, in: *Ext. Abstr. of Papers presented at VIII All-Union School-Seminar "Modern Problems of Gas Dynamics and Heat and Mass Transfer and Ways of Improving the Efficiency of Power Plants" headed by A. I. Leont'ev* [in Russian], Pt. 1, MGTU, Moscow (1991), pp. 38–39.